JOURNAL OF MATERIALS SCIENCE **37** (2002) 1541 – 1546

Sintering of 6H(α)-SiC and 3C(β)-SiC powders with B_4C and C additives

H. N. YOSHIMURA, A. C. DA CRUZ
Chemistry Division, Institute of Technological Research of the State of São Paulo, São Paulo, SP, Brazil
E-mail: hnyoshim@ipt.br

Y. ZHOU
Ceramic Science Department, National Industrial Research Institute of Nagoya, Nagoya, Japan

H. TANAKA
National Institute for Research in Inorganic Materials, Tsukuba, Ibaraki, Japan

The sintering behavior of three fine industrial SiC powders (two 6H(α)-type and one 3C(β)-type) has been comparatively investigated. The powders were pressureless sintered with B_4C and C additives between 1950°C and 2250°C in a high temperature dilatometer with flowing Ar atmosphere. The densification and shrinkage rate curves, polytype content, and grain growth were correlated with physical and chemical characteristics of starting powders. One of 6H(α)-type powders presented good sinterability only after extensive milling, even though it presented small average particle size, narrow particle size distribution and high specific surface area. The main difference in densification behavior among powders was the narrower shrinkage rate curve of β-SiC powder, with its maximum shifted to higher temperature. Grain growth and phase transformation simultaneously occurred. In α-SiC, 6H polytype partially transformed to 4H. This transformation was favored by aluminum impurity and resulted in a microstructure with more elongated grains. In β-SiC, 3C transformed mainly to 6H, 15R and 4H, introducing many stacking faults which resulted in elongated SiC grains.

1. Introduction

Silicon carbide (SiC) ceramics have been used in industry because of their favorable properties such as high elastic modulus and hardness, good thermal and chemical stability, high thermal conductivity, and relatively low thermal expansion coefficient. Some applications include, mechanical seals for liquid pumps and annealing furnace furniture for integrated-circuit (IC) wafers. Industrially, SiC ceramics are classified as either α-type phase (6H and non-cubic phases) or β-type phase (cubic 3C).

SiC is a highly covalent bonded material. Presently, the production of high density sintered SiC products cannot be achieved without using sintering additives. Pressureless sintering of β-SiC with B and C, probably in the solid state, was first announced by Prochazka in 1975 [1]. He proposed that C acts as a deoxidizing agent (reducing SiO_2 which is present at the surface of SiC particles), and dissolved B segregates to grain boundaries and increases atom diffusivity. The C effect would rise the interfacial energy, and the B effect would decrease the grain boundary energy, both would favor densification during SiC sintering.

Since Prochazka's work, many developments and advances in understanding pressureless sintering of SiC have been made. New additives, optimization of additive contents, the way additives are introduced, the effect of atmosphere, the understanding of polytype stability, and the importance of carbon in solution are some examples [2–5].

Other additive systems based on the B-C system have been investigated; the B-C-Al system being the most prominent. The benefits of adding Al atoms are: i) the decrease of sintering temperature, possibly assisted by the presence of a liquid phase even in the absence of oxygen [6]; and ii) to generate a more elongated and interlocked grain structure by favoring the 6H to 4H polytype transformation which tends to increase the fracture toughness of SiC [6].

Liquid phase sintering with oxide additives, like Al_2O_3 and Y_2O_3, has also been extensively studied, mainly addressed to lowering SiC sintering temperature. In these systems, the microstructure of SiC has been controlled by the addition of seeds which promote the formation of elongated grains in an equiaxed grain matrix [7, 8]. A problem associated with oxide additive systems is the high mass loss during normal sintering (due to the formation of volatile SiO and CO gases) which makes difficult to achieve full densification [9].

The objective of the present study was to investigate the densification behavior of three kinds of fine commercial SiC powders. The difference in the densification behavior, density, and microstructure of sintered materials were correlated with the characteristics of starting powder (α or β-type, and impurity level) and, in case of one of the powders investigated, to additional milling time.

2. Experimental

Three industrially synthesized fine SiC powders were used as raw materials: two 6H(α)-type, named α-1 and α-2, and one 3C(β)-SiC. These powders were analyzed via chemical analysis (free carbon, free SiO_2, aluminum, and iron), in accordance with Japanese Industrial Standard JIS-R1616. Their particle size distribution was determined by laser scattering method, and their specific surface area by nitrogen adsorption.

Each SiC powder was wet mixed in ethanol with 0.4 wt% B_4C powder (Cerac Inc. Milwaukee, WI), 5 wt% of phenolic resin (Dainipponn Ink & Chemicals Co., Saitama, Japan), yielding after decomposition the equivalent of $\sim$1.8 wt% C, and 2% over the total mass of poly(ethylene glycol) used as a binder. Mixing was carried out in a planetary mill during 8 h, using SiC milling media to avoid contamination. Only the α-2 powder was further milled for 100 h in an attempt to improve its sinterability (this particular preparation of α-2 powder to be also referred to as α-2-milled). Dried and granulated powders were cold isostaticaly pressed at 200 MPa to produce green bodies with approximately $5 \times 6 \times 20$ mm^3. The samples were sintered in two stages using a high temperature dilatometer (Netsch 402 E/7, Selb Germany) inside a graphite crucible: first they were heat-treated under vacuum at 1500°C for 30 min. (minimum pressure of $\sim 10^{-1}$ Pa); following, they were sintered at normal pressure between 1950°C and 2250°C for 30 min. in flowing Ar atmosphere (at a heating rate of 8°C/min.).

The density of green bodies and some sintered samples which presented low densities was determined by mass and size measurements. The density of the most sintered samples was determined by liquid (water) immersion method (Archimedes' Principle). The sintered samples were surface polished until 1 μm diamond. The amounts of 2H, 3C, 4H, 6H, and 15R SiC polytypes were determined using X-ray diffraction analysis and a data-fitting method proposed by one of the authors [10]. The microstructure of the polished and chemically etched surface [boiling method using Murakami's reagent, a saturated solution of equal parts of NaOH and $K_3Fe(CN)_6$] of each specimen was observed by Scanning Electron Microscopy (SEM).

3. Results and discussion

The characteristics of SiC powders are presented in Table 1. Powders α-1 and α-2 presented almost the same level of free-carbon and iron impurities, but powder α-2 presented higher contents of free-silica and aluminum impurities. Both α-1 and α-2 powders were constituted mainly by non-cubic polytypes (predominantly 6H), but powder α-2 presented higher contents of polytype impurities (2H, 3C, and 4H). Compared with 6H(α) powders, powder β presented higher free carbon and aluminum contents, and was constituted mainly by cubic 3C polytype. With respect to granulometry, powder α-1 presented larger average particle size and broader, possibly bimodal, particle size distribution. Although powders α-2 and β presented almost the same particle size distribution, powder β presented higher surface area. SEM analysis showed that powder α-2, compared with powders α-1 and β, presented particles with sharper and more angular morphology and smooth cleaved surfaces, indicative of intense comminution during powder preparation.

Green densities of compacts prepared with powders α-1, α-2, and β were $\sim$65%TD (theoretical density), $\sim$55%TD and $\sim$60%TD, respectively. Possibly, the better compaction of powder α-1 (which resulted in higher green density) was related with its larger and broader particle size distribution, and, on the other hand, the worst compaction of powder α-2 (which resulted in lower green density) seems to be a consequence of its narrow particle size distribution and angular particle morphology. Additional 100 h milling of powder α-2 caused no appreciable change on particle size distribution, neither on green density.

Fig. 1 presents the shrinkage curves of samples prepared from powder β sintered at different holding temperatures. The maximum shrinkage attained during heating (without considering holding step) was at 2150°C. Similar results were observed on shrinkage curves of samples prepared from powder α-1. The first stage of sintering (1500°C, 30 min., under vacuum) caused negligible shrinkage on all samples.

Fig. 2 presents the results of densification curves (estimated from shrinkage data) and shrinkage rate curves of samples prepared from powders α-1, α-2, α-2-milled, and β sintered at 2150°C. While the sample first prepared from powder α-2 presented low densification, further milling of 100 h improved sinterability, resulting in a density comparable to samples α-1 and β

TABLE I Powder characteristics

	Chemical analysis (mass %)				Polytype content (%)					Particle size (μm)			S
Powder	F. C	F. SiO_2	Fe	Al	2H	3C	4H	6H	15R	D_{10}	D_{50}	D_{90}	(m^2/g)
α-1	0.49	0.34	0.030	0.004	0	2	0	91	7	0.34	0.71	2.33	13.3
α-2	0.30	0.92	0.026	0.016	2	5	1	85	7	0.34	0.53	0.94	14.6
β	0.81	0.37	0.035	0.044	5	94	0	0	1	0.34	0.50	0.93	19.1

Notes: F.—free; S—specific surface area (BET method).

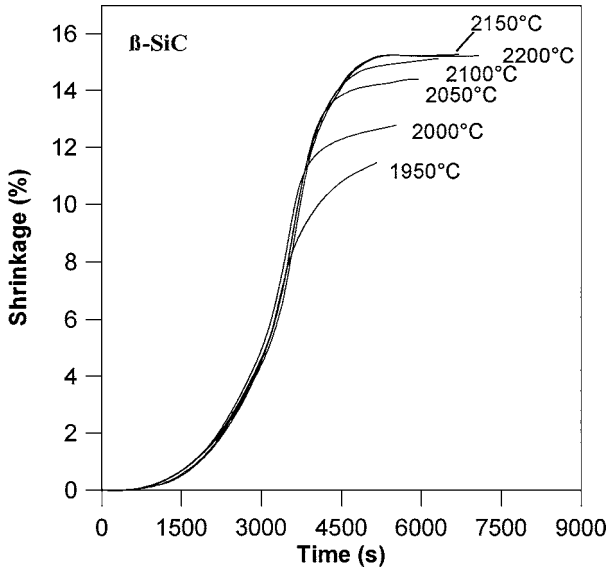

Figure 1 Shrinkage curves of sample β sintered at different holding temperatures.

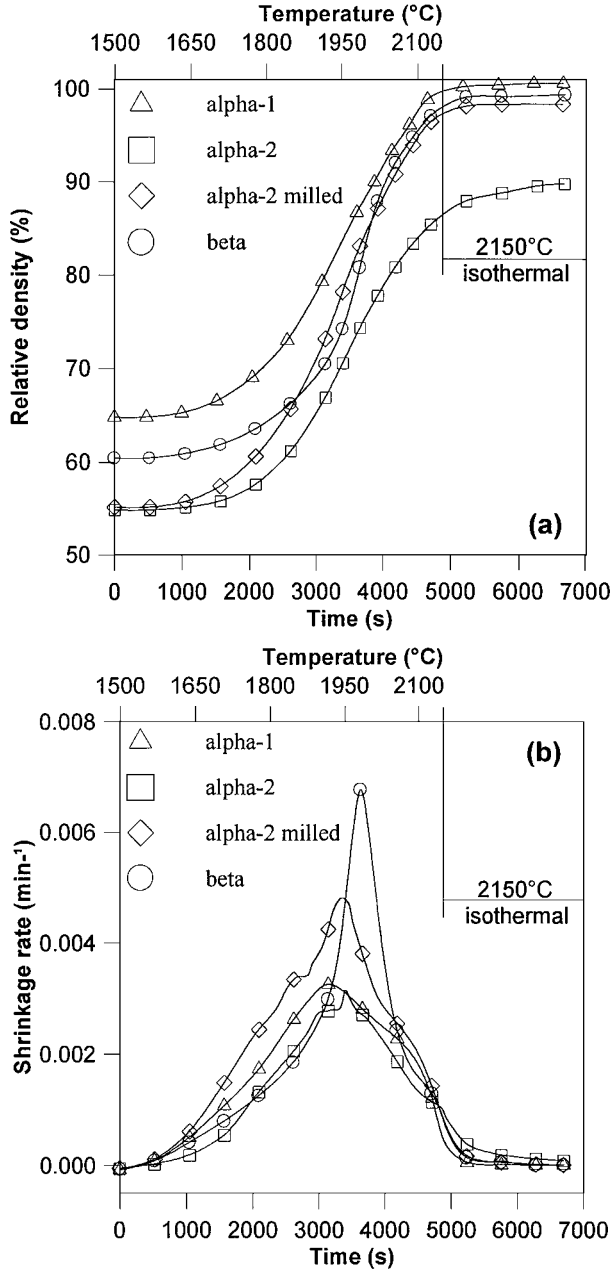

Figure 2 Relative density (a) and shrinkage rate (b) as a function of sintering time of samples α-1, α-2, α-2-milled, and β.

(Fig. 2a). All samples presented significant shrinkage (mainly between 1650°C and 2150°C), but the temperature of maximum shrinkage rate varied among samples (1915°C, 1940°C, 1930°C and 1980°C for samples α-1, α-2, α-2-milled and β, respectively).

The improvement on sinterability of powder α-2 by milling was accompanied by an increase on shrinkage rate, with almost no shift on peak temperature (Fig. 2b). Although powder α-2 had smaller average particle size, narrower particle size distribution, and higher specific surface area (Table I), it presented poorer sinterability than powder α-1. The low compressibility of this powder seems to have contributed to this result. In another set of experiments (not shown here), it was observed that the density of sintered samples prepared from powder α-2 was strongly affected by the density of green compacts. Another reason for the poor sinterability of powder α-2 could be related with its high content of silica impurity (Table I). In a previous work [11] it was observed that 6H-SiC powders which contained the most silica impurity required the greatest amount of boron additive for complete densification, since silica seems to react with boron, reducing its effect on sintering. The beneficial effect of milling on the improvement of powder α-2 sinterability is not clear. One possible explanation could be a consequent increase of the homogeneity of the distribution of additives which, by this time, might have increased their effectiveness.

The main difference on densification behavior among powders which presented high sinterability (α-1, α-2-milled, and β), was the steeper densification curve of powder β (Fig. 2a), with its shrinkage rate maximum shifted to higher temperature and with highest peak of all (Fig. 2b). This result indicates that more care on heating cycle of sintering of 3C(β) powders should be necessary to avoid high temperature gradients between core and surface of thick bodies.

Fig. 3 presents bulk densities of samples sintered for 30 min between 1950°C and 2250°C. The density of the samples prepared from powders α-1 and β (from now on referred to as samples α-1 and β,

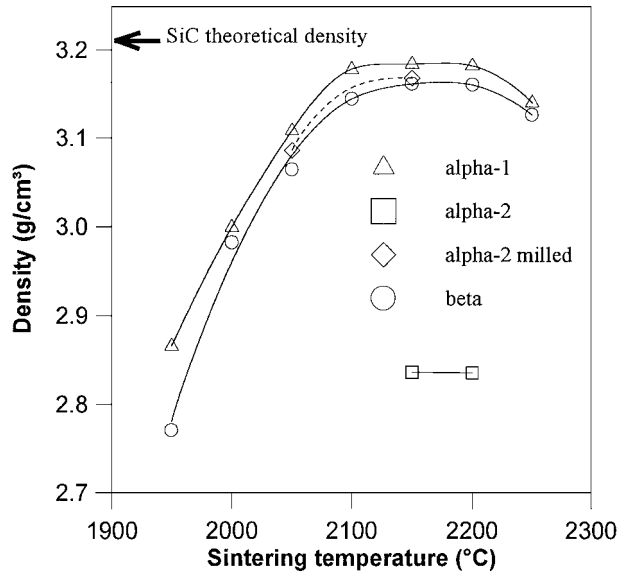

Figure 3 Bulk densities of samples α-1, α-2, α-2-milled, and β sintered for 30 min. between 1950°C and 2250°C.

and so on) steadily increased with increasing temperature until around 2100°C, remained almost constant until around 2200°C, and at 2250°C presented a small drop of around one percent. For all the temperatures, sample α-1 presented a higher density than sample β, the difference varying between 0.4% and 1.3% in the range of 2000°C to 2250°C (at 1950°C the difference was ~3.0%). The highest densities determined for samples α-1, α-2-milled and β were 3.184 g/cm^3 (99.2%TD), 3.168 g/cm^3 (98.7%TD) and 3.161 g/cm^3 (98.5%TD), respectively (all sintered at 2150°C). Sample α-2 presented low density even when sintered at 2200°C (Fig. 3).

Fig. 4 shows the polytype content as a function of sintering temperature (as reference, results of starting powders are also indicated). Up to 2200°C, sample α-1 presented ~90% of 6H polytype and a slow increase of 4H polytype content; at 2250°C its 6H content dropped to ~70% and 4H content abruptly increased to ~22% (Fig. 4a). About 5% of 15R polytype and some traces of 2H and 3C polytypes were also observed. Samples α-2 and α-2-milled presented slightly lower 6H polytype content and higher 4H polytype content than sample α-1 (Fig. 4a). Between 1950°C and 2250°C, sample β presented a strong decrease of 3C polytype content (from ~90% to ~20%); at the same time, non-cubic polytypes have increased, mainly 6H (from ~1% to ~50%), followed by 15R (from ~4% to ~20%), and 4H (from ~1% to ~10%). Some traces (~5%) of 2H polytype were observed until 2100°C (Fig. 4b). These results showed that between 1950°C and 2250°C sample α-1 was more stable than sample β with respect to polytypic transformation (Fig. 4).

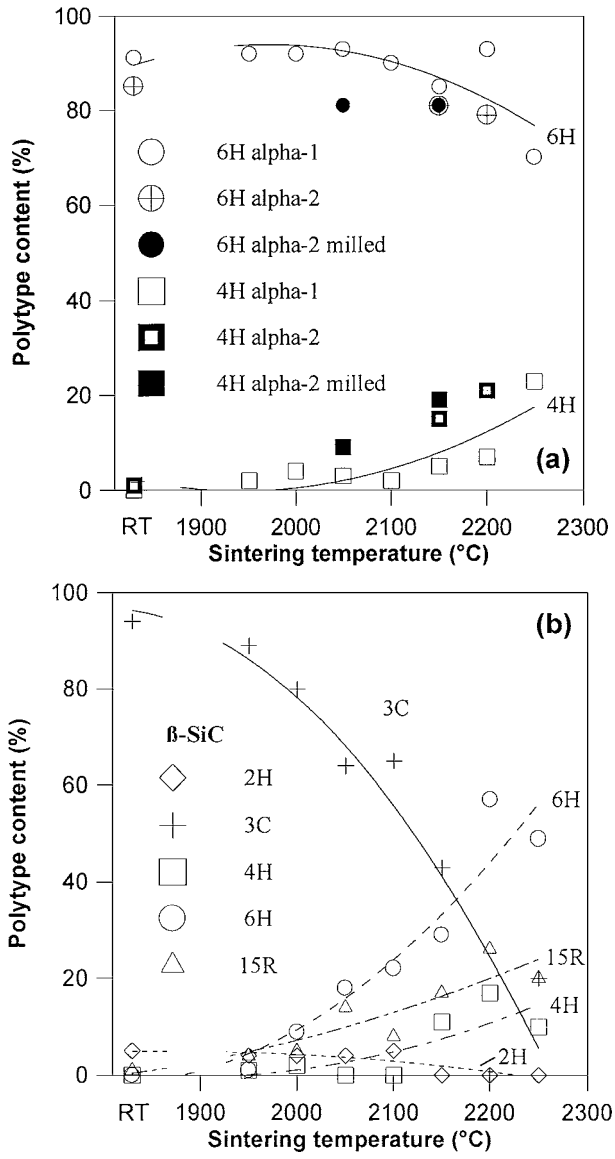

Figure 4 Polytype content as a function of sintering temperature of: (a) samples α-1, α-2, and α-2-milled; and (b) sample β (RT-room temperature).

Fig. 5 presents some micrographs of sintered samples. Up to 2150°C, sample α-1 presented a relatively homogeneous microstructure with near-equiaxial-shape grains (Fig. 5a). At 2200°C, abnormal grain growth (AGG) resulted in a bimodal grain size distribution, with large platelike grain (Fig. 5b). At 2250°C, a coarse microstructure having predominantly large platelike grains was observed. AGG occurred simultaneously with the phase transformation of 6H to 4H polytype (Fig. 4a).

Sample α-2 sintered at 2150°C and 2200°C presented elongated grains with large pores, generally located at grain boundaries (Fig. 5c). Sample α-2-milled sintered at 2150°C presented low porosity and a microstructure constituted mainly of elongated grains, with some large platelike grains (Fig. 5d). Sample α-2, which presented little densification, showed more grain growth than the sample α-2-milled (Fig. 5c and d). Up to 2150°C, samples α-2 and α-2-milled presented microstructures with more elongated grains than sample α-1 (Fig. 5a, c, and d). This seems to be related with the higher content of aluminum impurity on starting powder α-2, compared with powder α-1 (Table I). In a previous work [11] it was observed that a 6H-SiC powder that contained the highest level of aluminum impurity exhibited partial transformation of 6H to 4H polytype, which seemed to have induced elongated grain growth. Aluminum atoms are thought to have stabilized 4H polytype and accelerated the transformation of 6H polytype during sintering. The higher content of 4H polytype in sample α-2, compared with sample α-1, can be observed in Fig. 4a. Because the starting powder α-2 presented small amounts of 2H, 3C, and 4H (Table I), it is possible that these polytype impurities acted as embryos at high temperatures (in which transformation began).

Between 1950°C and 2150°C, sample β presented relatively homogenous microstructures containing elongated grains with some large platelike grains (Fig. 5e). At 2200°C and 2250°C, dramatic changes occurred towards a microstructure containing very large irregular grains (Fig. 5f). The transformed β-SiC (3C to 6H, 15R and 4H, Fig. 4b) seemed to have many defects, like stacking faults, which could be observed in SEM analysis (Fig. 5e). This result indicated that either the partial transformation or stacking faults in transformed 3C SiC made the SiC grains elongate.

In general, samples with good sinterability (α-1, α-2-milled and β) presented relative fine homogeneous microstructures with normal grain growth up to 2150°C

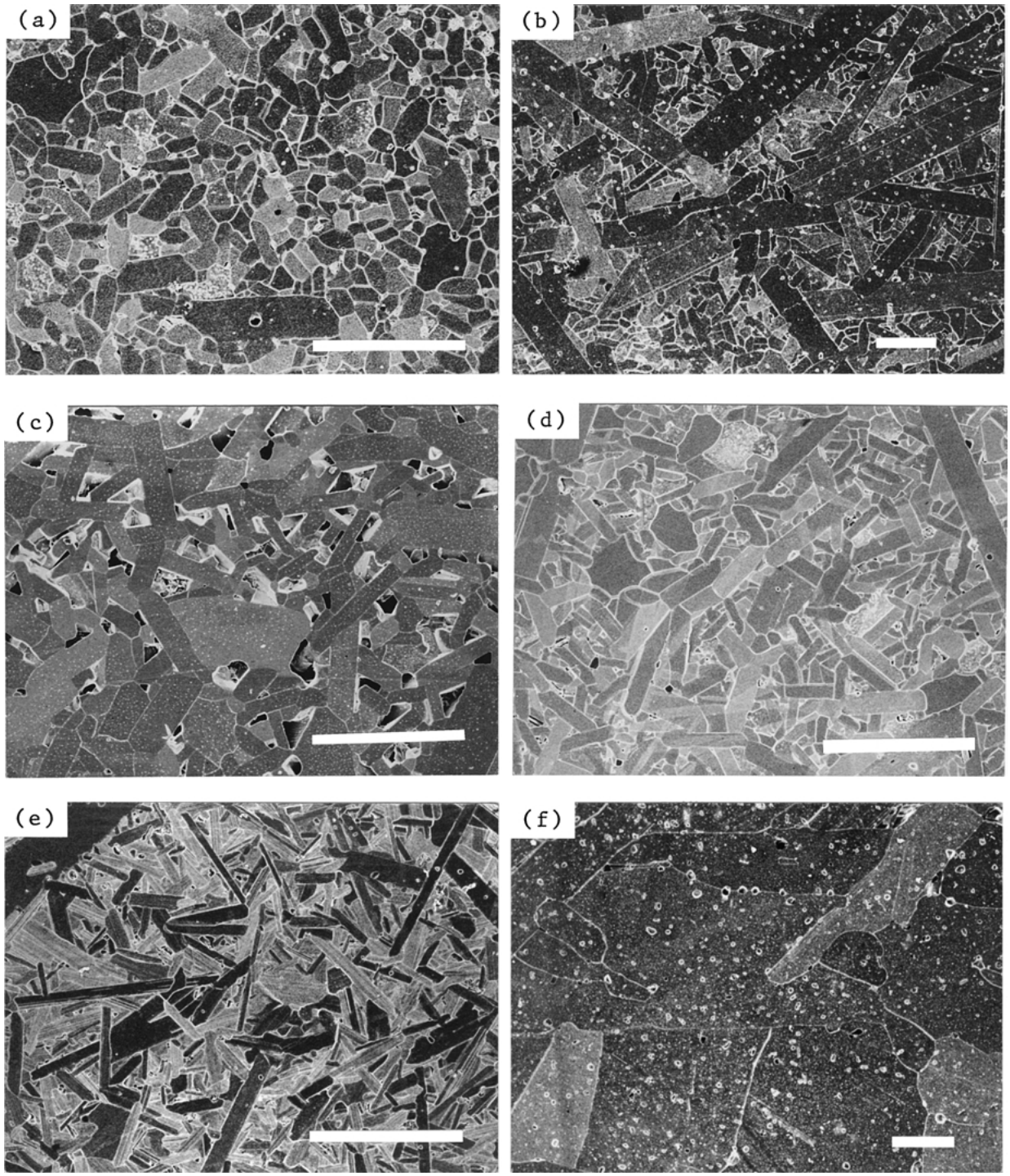

Figure 5 SEM of the chemically etched surfaces of samples sintered at different temperatures: (a) α-1 at 2150°C; (b) α-1 at 2200°C; (c) α-2 at 2150°C; (d) α-2-milled at 2150°C; (e) β at 2150°C; and (f) β at 2200°C (Bar = 20 μm).

(when maximum densification was achieved). Above this temperature, AGG occurred resulting in coarse microstructures (Fig. 5).

The drop on density of samples α-1 and β at 2250°C observed in Fig. 4 will now be interpreted. The lowering of density at high sintering temperatures was also observed in a previous work by one of the authors [10]. The samples α-1 and β, sintered at 2250°C, presented many large pore like defects inside abnormally grown grains, or at the grain-boundaries (Fig. 5b and f). Usually, when AGG takes place before the sample have achieved total densification, it results in a microstructure having large grains with entrapped pores which practically stop further densification [12]. However, in this study it seems that AGG was not direct responsible for the density decrease at 2250°C, as the maximum density was achieved at about 2150°C (Fig. 1) and AGG occurred above this temperature (Fig. 5). The decrease of the SiC density at high sintering temperature seems to be better explained by gas expansion due to pore growth, and also possibly by pore precipitation. It was pointed out by Coble [13] that during pore coalescence the gas moving from small to large pores tends to expand, once the equilibrium pressure in larger pores is lower. By the same reason, the quantity of gas in solution decreases, which can intensify the decrease in

density or 'bloating' effect [13]. Indeed, a slightly linear expansion was detected in the shrinkage curve of sample α-1, at a temperature near 2250°C.

The results gathered in the present investigation showed that SiC powders, with good sinterability, pressureless sintered with B and C additives between 1950°C and 2250°C, presented similar densification behavior (Fig. 3), and similar tendency to the occurrence of abnormal grain growth, irrespective of polytypic nature of starting powder.

4. Summary and conclusions

Three fine SiC powders, two 6H(α)-type, named α-1 and α-2, and one 3C(β)-SiC, were pressureless sintered with 0.4% B_4C and ~1.8% C, between 1950°C and 2250°C in a high temperature dilatometer with flowing Ar atmosphere. The effect of milling on sintering was observed in case of powder α-2, which presented good sinterability only after extensive milling. The main difference on densification behavior among powders was the narrower shrinkage rate curve of powder β, with its maximum shifted to higher temperature. Grain growth and phase transformation simultaneously occurred. In α-SiC, 6H polytype tends to transform to 4H. Aluminum contamination favored the 6H to 4H transformation. The polytype impurities (2H, 3C, and 4H) present in powder α-2 might have acted as embryos for this transformation at high temperature, producing a microstructure with more elongated grains. In β-SiC, 3C tends to partially transform to 6H, 15R, and 4H. The transformed β-SiC seems to have defects, like stacking faults. Partial transformation or stacking faults in transformed 3C SiC caused the SiC grains to elongate.

Acknowledgement

The authors thank the Japan International Cooperation Agency-JICA for the financial support of the present research.

References

1. S. PROCHAZKA, in Proceedings of the 6th Symposium on Special Ceramics, Stoke-on-Trent, July 1974, edited by P. Popper (British Ceram. Res. Assoc., Stoke-on-Trent, 1975) p. 171.
2. H. TANAKA, in "Silicon Carbide Ceramics I," edited by S. Somiya and Y. Inomata (Elsevier, London, 1991) p. 213.
3. R. M. WILLIAM, B. N. JUTERBOCK, C. R. PETERS and T. J. WHALEN, *J. Amer. Ceram. Soc.* **67** (1984) C-62.
4. B. W. KIBBEL and A. H. HEUER, *ibid.* **72** (1989) 517.
5. W. BUCKER, H. LANDFEEMANN and H. HAUSNER, *Powder Metallurgy International* **13** (1991) 37.
6. Y. ZHOU, H. TANAKA, S. OTANI and Y. BANDO, *J. Amer. Ceram. Soc.* **82** (1999) 1959.
7. F. F. LANGE, *J. Mater. Sci.* **10** (1975) 314.
8. N. PADTURE, *J. Amer. Ceram. Soc.* **77** (1994) 519.
9. T. GRANDE, H. SOMMERSET, E. HAGEN, K. WIIK and M. A. EINARSRUD, *ibid.* **80** (1997) 1047.
10. H. TANAKA and N. IYI, *ibid.* **78** (1995) 1223.
11. H. TANAKA, H. N. YOSHIMURA, S. OTANI, Y. ZHOU and M. TORIYAMA, *ibid.* **83** (2000) 226.
12. J. E. BURKE, *ibid.* **40** (1957) 80.
13. R. L. COBLE, *ibid.* **45** (1962) 123.

Received 17 April
and accepted 21 December 2001